HOLOGRAPHIC GENERATION OF BUBBLE GRATINGS AT LIQUID–GLASS INTERFACES AND THE DYNAMICS OF BUBBLES ON SURFACES

Gregory EYRING and M.D. FAYER
Department of Chemistry, Stanford University, Stanford, California 94305, USA

Received 18 March 1983; in final form 28 April 1983

Intense diffraction from a periodic array of microscopic bubbles is reported. The bubbles are generated by 100 ps, 1.06 μm pulses from a Nd : YAG laser which are crossed at a liquid–dielectric interface. The time dependence of the diffraction yields information on surface bubble expansion, contraction, and migration. The mechanism for the production of the bubble gratings is described.

1. Introduction

In this letter we report the observation of intense diffraction from holographic gratings of microscopic bubbles at a glass–liquid interface. The bubbles are produced in the intensity peaks of the interference pattern generated by a pair of picosecond laser pulses crossed at the interface. Because of the large difference in the refractive index between the gas and the liquid, this bubble grating, though very thin (≈1 μm), results in efficient diffraction of a variably delayed probe pulse brought in at the Bragg angle. By examining the dependence of this diffraction on probe pulse delay between 10^{-11} and 10^{1} s, a variety of dynamical properties of the surface bubbles can be studied. These are the expansion and contraction of the bubbles, and their migration on the surface.

Previously, bubbles have been produced by single laser beams in bulk liquids [1–7], and this effect has been used to study vapor bubble dynamics [7]. The bubbles are typically nucleated at the surfaces of impurity particles which are strongly heated by the absorption of light. Our results suggest that there is a mechanism by which the optical radiation causes particles from the liquid to be deposited on the glass surface. These surface particles serve as nucleation sites for the production of the bubble grating. We found that an appropriate optical pulse sequence could then remove these particles from the surface and eliminate the probe pulse diffraction.

2. Experimental

The experimental apparatus is diagrammed in fig. 1, and is described in more detail elsewhere [8,9]. The laser is a continuously pumped Nd : YAG system which

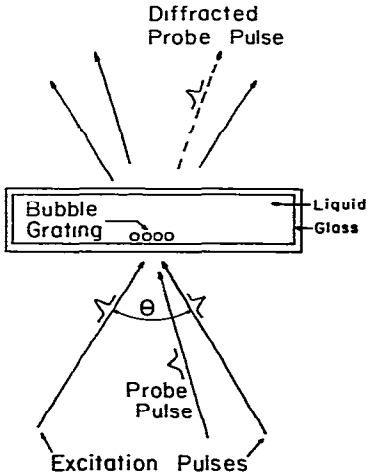

Fig. 1. Schematic illustration of the experimental geometry for the production and detection of bubble gratings. Two 100 ps, 1.06 μm excitation pulses are crossed at the interface between a glass cuvette and a liquid. Stripes of microscopic bubbles are generated in the intensity peaks of the resulting interference pattern. This bubble grating causes strong diffraction of a variably delayed, 0.532 μm probe pulse brought in at the Bragg angle.

0 009-2614/83/0000–0000/S 03.00

is acousto-optically mode-locked and Q-switched to produce 1.06 μm pulses at 400 Hz. The output is a train of some 40 mode-locked pulses of width $\approx$100 ps, separated by 9 ns. An $\approx$50 μJ pulse from the center of the train is selected by a Pockels cell. In some experiments, the Pockels cell window was widened to select two pulses, 9 ns apart. A small portion of the IR single pulse is frequency doubled using CD^*A to give an $\approx$1 μJ probe at 532 nm. The remainder is beam-split to give two $\approx$15 μJ pulses which, after traveling equal path lengths, are crossed at an angle θ at the interface between a glass or quartz cell and a liquid. The interface is thus exposed to a sinusoidally varying pattern of intensity peaks and nulls produced by the interference between the IR excitation beams. The fringe spacing is given by

$$\Lambda = \lambda/2 \sin(\theta/2), \quad (1)$$

where λ is the laser wavelength. In a typical case, θ = 26°, λ = 1.06 μm yields a value of 2.36 μm for Λ. The interaction region of the IR beams is probed at the Bragg angle with the 532 nm pulse which could be timed to arrive continuously from 2 ns before, to 16 ns after, the IR excitation, using an optical delay line. Spot sizes of the excitation and probe beams were 100 and 50 μm, respectively. Most of our experiments were done on benzyl benzoate in a 1 mm glass absorption cuvette, but this was largely a matter of convenience, since the effect was observed in many other liquids, including melted benzophenone and biphenyl [8].

3. Results and discussion

The experiment was initiated by exposing the glass–liquid interface to the crossed IR and probe beams. At first, no probe diffraction could be observed. After about one minute however, a first-order diffraction spot appeared which rapidly increased its intensity over several seconds until it reached a few percent of the transmitted probe intensity. The onset time was independent of whether the probe delay was a few nanoseconds or a few milliseconds relative to the excitation. At this point, second- and third-order spots could be observed, though they were considerably weaker. If exposure to the IR beams was continued, the diffraction was interrupted at $\approx$15 s intervals by the formation of $\approx$40 μm diameter bubbles which were released from the glass at the spot of laser irradiation and floated slowly to the surface of the liquid.

When the sample was translated more than one spot diameter to the right or left, no diffraction could be seen for at least a minute. After returning to the original spot, however, intense diffraction was found immediately. Thus, the sample "remembered" where it had previously diffracted light. The memory was not a grating in itself since no diffraction was observed when only the probe beam was present. Instead, it consisted of a tendency, or "predisposition", to form a grating very rapidly when the crossed excitation beams were turned on. If the sample was left undisturbed, this memory persisted indefinitely. However, we found that by exposing the predisposed spot to a pulse sequence formed by selecting two adjacent pulses from the mode-locked pulse train, we could reversibly remove the ability of the sample to diffract the probe. That is, by changing back and forth between a single pulse (beam-split and recombined to form an interference pattern) and a pair of identical pulses separated by 9 ns and traveling along the same paths, we could alternately create and erase the tendency to diffract light. A fresh sample spot exposed only to the double-pulse sequence neither diffracted light nor produced any visible bubbles. Thus, the double pulse sequence was able to reverse the effect of the normal grating excitation.

The observation that relatively large bubbles are periodically released from the laser spot implies that a grating of microscopic bubbles is the origin of the diffraction. The grating thickness can be estimated assuming that a large bubble is released when the smaller bubbles approach uniform coverage of the laser spot. For the observed 40 μm diameter bubble and a spot size of $\approx$100 μm, one obtains a diameter of $\approx$1 μm for the microbubbles. This estimate is consistent with the diffusion measurements discussed below. The large difference in refractive index, Δn = 0.3–0.5, between gas or vapor and liquid accounts for the relatively high diffraction efficiency (up to 10% in the +1 order) from a grating only 1 μm thick.

The nature of the diffracted light was examined more quantitatively using a fast PIN photodiode and a Biomation model 805 waveform recorder. The character of the diffraction from a predisposed spot was found to be dramatically different depending on whether the grating was probed a few nanoseconds or a few milliseconds after the arrival of the excitation pulses.

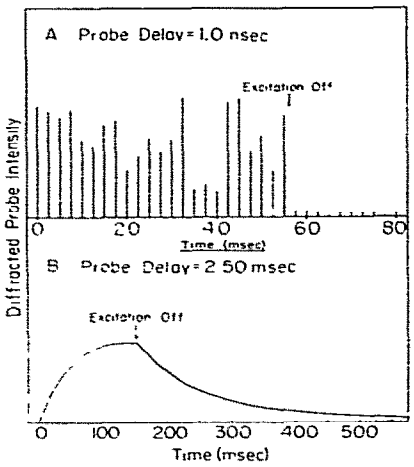

Fig. 2. Time course of the diffracted probe intensity at a predisposed spot on the glass–liquid interface when the bubble grating is probed 1 ns (A) and 2.5 ms (B) after the arrival of the crossed excitation pulses. The excitation pulses are turned on at $t = 0$ and blocked at the arrows. Each spike in A corresponds to an individual laser shot (400 Hz). The vertical scale in B is expanded by a factor of 10 relative to A. Since in B the shot-to-shot fluctuation in the diffraction is small, only the envelope of the diffracted probe pulses is depicted.

The millisecond delay was achieved by adjusting the optical delay line so that the probe arrived slightly before the excitation pulses (i.e. 2.5 ms after the previous excitation pulses for a 400 Hz repetition rate). Fig. 2A displays the diffracted light intensity of a series of shots for the case where the grating was probed 1 ns after the excitation. Intense diffraction was observed on the first shot and continued erratically until the excitation beams were blocked (arrow), after which a large fraction of the intensity disappeared before the next probe shot 2.5 ms later. A very different behavior was observed when the grating was probed 2.5 ms after the arrival of the excitation, as shown in fig. 2B. The overall first-order diffraction intensity was an order of magnitude weaker, so the vertical scale is expanded by a factor of 10 relative to 2A. The time scale has been contracted in order to show the behavior of the grating long after the excitation beams are blocked. Only the envelope of the diffracted probe pulses is drawn. Notice that in this case the diffraction is much more stable from shot to shot, taking 15–25 shots to build up to a steady state. When the excitation beams are blocked (arrow), the intensity decays exponentially to zero over several hundred milliseconds.

These data are readily explained by a laser-induced bubble grating as follows. The excitation pulses are partially absorbed by small particles attached to the surface which lie in the grating peaks. For the intensities used, we estimate that the temperature of an opaque particle could rise from several hundred to several thousand degrees in a single shot. This local heating vaporizes and degasses the surrounding liquid, producing a grating of expanding bubbles containing both vapor and non-condensable gas. The presence of these hot, expanded bubbles gives rise to the intense and erratic diffraction in fig. 2A. After a time short compared with the repetition rate, the vapor condenses, leaving smaller residual gas bubbles having a lifetime of many seconds. The risetime of the diffraction in 2B can be explained as follows. The formation of gas bubbles results in a depletion of dissolved gas in the illuminated volume, which is replenished by diffusion of gas molecules from the surrounding liquid. Thus the bubble production rate reaches a steady-state value after 15–25 shots.

When the excitation beams are blocked, the concentrations of microbubbles in the peaks and nulls become equal by migration of the bubbles on the surface. If this migration corresponds to simple diffusion, the diffraction intensity will decay exponentially with a time which depends on the fringe spacing [10]:

$$I(t) = I_0 \exp[-2(2\pi/\Lambda)^2 Dt], \quad (2)$$

where D is the diffusion constant. Measurements of these decays at different fringe spacings should result in different decay rates, but the same diffusion constant. In fig. 3, the decays observed at two fringe spacings are plotted. Within experimental error, these yield the same value for $D = (1.8 \pm 0.6) \times 10^{-9}$ cm^2/s. The fact that both decays are nearly exponential suggests that the microbubbles are relatively uniform in size.

From kinetic theory, the diffusion constant of a particle undergoing brownian motion is

$$D = 6kT/f, \quad (3)$$

where f is the friction coefficient. For a spherical particle of radius r immersed in a medium of viscosity η, f is given by Stokes' equation:

$$f = 6\pi\eta r. \quad (4)$$

If we neglect the interaction of the bubbles with the surface, these formulas can be used to verify that the bubble diffusion constant measured above is the right order

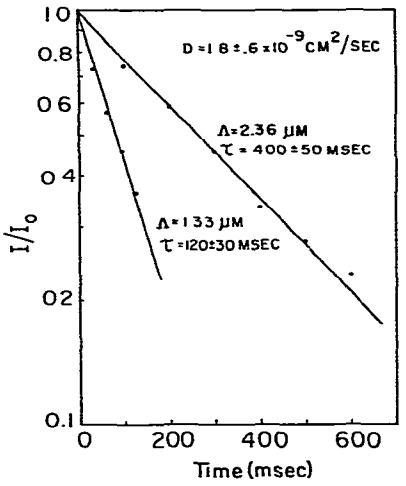

Fig. 3. The intensity of the +1 order probe diffraction versus time after blocking the excitation beams. The points are taken from curves like that in 2B (following the arrow) for two different values of the fringe spacing Λ. Both decays are exponential and, while their time constants τ are very different, the calculated diffusion constant, D, is the same. This demonstrates that the loss of diffracting power is due to the diffusion of microscopic gas bubbles from the grating peaks to the nulls.

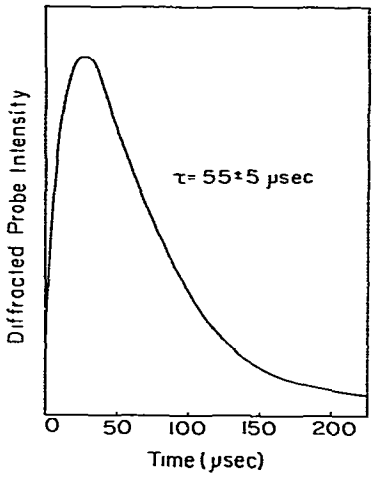

Fig. 4. The first-order diffraction of a cw probe beam versus time following a single shot of the IR grating excitation on a predisposed spot. The true rising edge (350 ps) is not resolved in this experiment. The decay time is 55 ± 5 μs. This reflects the time required for the hot, expanded bubbles to cool and contract.

of magnitude. Taking $T = 300$ K, $\eta = 8.5 \times 10^{-2}$ P for benzyl benzoate and r in the range 0.1—1 μm, we obtain D in the range 10^{-8}—10^{-9} cm²/s. This agrees well with our experimental value.

The maximum possible diameter of the microbubbles is the grating fringe spacing Λ. The data shown in fig. 3, however, suggest that their actual size is independent of Λ, since the diffusion constant, which varies inversely as the bubble radius [eqs. (3) and (4)] was the same for two different fringe spacings. Thus the smaller value of Λ = 1.33 μm, gives an upper limit to the diameter of the microbubbles.

The onset and decay times of the intense, erratic diffraction were determined in separate experiments. The time delay between the point where the probe and excitation beams were simultaneously present at the interface ($t = 0$) and when the intense diffraction was first observed, was measured with the optical delay line to be 350 ± 50 ps. This is roughly the time which would be required for a bubble expanding at the speed of sound in benzyl benzoate (≈2 × 10⁵ cm/s) to reach a radius of 1 μm. In order to measure the loss of diffraction efficiency caused by the collapse of the hot bubbles, it was necessary to probe the grating with a cw beam so that diffraction could be followed continuously on a microsecond time scale. For this purpose we used an ≈50 mW, 590 nm beam from an argon-ion-pumped rhodamine-6G dye laser as a probe. The time course of the diffraction from a single shot of the IR grating is shown in fig. 4. For these experiments, the recording instrument rise time was ≈4 μs. Therefore, the 350 ps rising edge of the diffraction is not resolved. The decay is approximately exponential with a time constant of 55 ± 5 μs. We propose that this is the time required for the expanded bubbles to lose heat to their surroundings, and for the vapor to condense.

The origin of the diffraction predisposition on the glass surface is evidently the deposition of particulate nucleation sites by the laser beam. After irradiation for at least 30 min, we could observe a faint residue on the glass surface under a microscope at 100X magnification. This could occur, for example, if dust floating in the vicinity of the laser spot were drawn to the surface and attached. This view is supported by the observation that if the surface was thoroughly cleaned and the liqui carefully filtered through a pore size of 0.2 μm, no diffraction could be generated. Subsequent addition of small particles to the cleaned liquid would regenerate

the effect. The mechanism by which the double-pulse sequence erases the tendency to diffract light would then be to clean the dust particles from the surface, and to prevent new ones from attaching. We are currently conducting experiments to determine whether the additional heat deposited by the second pulse could cause mechanical cleaning of the surface or whether laser-induced charge separation and recombination processes are involved. This will be discussed in greater detail elsewhere [8].

4. Concluding remarks

In summary, we have found that it is possible to generate bubble gratings ≈ 1 μm thick at a liquid–dielectric interface which diffract light with efficiencies up to 10%. The diffraction can be used to monitor bubble dynamics as well as diffusion on the surface. The tendency to form these gratings at a particular spot on the surface could be reversibly created or erased. Such laser-induced buble gratings may find application as extraordinarily thin, optically activated light gates.

Acknowledgement

GE would like to acknowledge the Public Health Service (1 F32 GM08011-01) for a postdoctoral fellowship. We would also like to thank the National Science Foundation (DMR 79-20380) for support of this research. MDF would like to acknowledge the Simon Guggenheim Memorial Foundation for fellowship support which contributed to this research.

References

[1] G.A. Askar'yan, A.M. Prokhorov, G.F. Chanturiya and G.P. Shipulo, Soviet Phys. JETP 17 (1963) 1463.
[2] G.A. Askar'yan, Soviet Phys. JETP 18 (1964) 555.
[3] R.C. Stamberg and D.E. Gillespie, J. Appl. Phys. 37 (1966) 459.
[4] A.A. Manenkov, Soviet Phys. Doklady 15 (1970) 155.
[5] A.A. Chastov and O.L. Lebedev, Soviet Phys. JETP 31 (1970) 455.
[6] G.A. Askar'yan and T.G. Rakhmanina, Soviet Phys. JETP 34 (1972) 639.
[7] W. Lauterborn, Appl. Phys. Letters 21 (1972) 27.
[8] G. Eyring and M.D. Fayer, to be published.
[9] A. Nelson and M.D. Fayer, J. Chem. Phys. 72 (1980) 5202.
[10] J.R. Salcedo, A.E. Siegman, D.D. Dlott and M.D. Fayer, Phys. Rev. Letters 41 (1978) 131.